

Cite this: *Soft Matter*, 2011, **7**, 6451

www.rsc.org/softmatter

PAPER

Spectral insights into gelation microdynamics of *N*-octyl-D-gluconamide in water†

Shengtong Sun and Peiyi Wu*

Received 30th March 2011, Accepted 27th April 2011

DOI: 10.1039/c1sm05548h

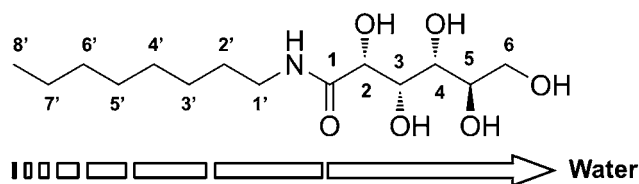
Near infrared spectroscopy in combination with two-dimensional correlation spectroscopy (2DCos) and perturbation correlation moving window (PCMW) technique is employed to illustrate the gelation microdynamic mechanism of hydrogelator *N*-octyl-D-gluconamide (8-GA), which can rapidly self-agglomerate into helical bilayer micellar fibers upon cooling from spherical micelles. Boltzmann fitting and PCMW easily determined the gelation temperature to be *ca.* 72 °C and the transition temperature range to be 70–75 °C. Moreover, band shifting and splitting phenomena can be observed for CH-related overtones, indicating the formation of much ordered and tight hydrophobic core from octyl tails. On the other hand, 2DCos was used to discern the sequential orders during the gelation process and concluded that all the group motions have a continuous transfer from the octyl tail to the chiral carbohydrate head followed by the final immobilization of the solvent, which meanwhile, is actually a continuous dehydration process from the hydrophobic core to the outer hydrophilic chiral head. The driving force of the gelation process in microdynamics can only be the dehydration process of hydrophobic octyl chains, but with final helical superstructures being stabilized by amide-associated hydrogen bonding and the “chiral bilayer effect” of carbohydrate heads.

1 Introduction

Over recent years, immense interests have been stimulated in low-molecular-weight (LMW) hydrogelators capable of gelling aqueous solvents due to their potential applications in templating nanostructured materials, controlled drug delivery, tissue engineering, and so on.¹ The gelation is generally considered to arise from nano- or microfibrils immobilizing and trapping solvents *via* surface tension.² Wherein, in contrast to inorganic and polymer gels, the solid 3D entangled network formed by LMW hydrogelators is linked solely *via* noncovalent interactions, such as hydrogen bonding, π – π stacking, coordination, hydrophobic and electrostatic interactions. Thus the gelation process is completely thermoreversible. Some basic rules have also been proposed to enable the design of new LMW gelators, *e.g.* the existence of strong intermolecular interactions to enforce 1D self-assembly, control of fiber-solvent energy to prevent crystallization and some other factors to intertwining the aggregates.³ In water, amphiphilic molecules with hydrophobic groups to promote aggregation and hydrophilic groups to provide solubility are most competent for hydrogelators.² Up to now, numerous amphiphile hydrogelators have been developed, such

as amphiphile lipids,⁴ sugar-based lipids,⁵ boloamphiphiles,⁶ gemini surfactants⁷ and two or three component systems.⁸

Chiral amphiphiles incorporating secondary amide groups often form fluid, spherical micelles in water above 80 °C, and quickly agglomerate upon cooling to give long helical micellar fibers with length-to-diameter ratio higher than 10⁴.⁹ For *N*-octylgluconamide (8-GA, as shown in Scheme 1), quadruple helices constructed from bilayer micellar cylinders can be observed by TEM, which is also the only known amphiphilic assembly of bimolecular thickness without a charged surface.¹⁰ However, the surface energy of such fibers was so large that they would rearrange quickly within several days to more stable crystals without curvature. Addition of small amounts of sodium dodecyl sulphate (SDS) proved to make it stable for years.¹¹ Moreover, curved fibers are stable only if the amphiphiles are enantiomers, and their racemates crystallize as planets.^{9c} This phenomenon is well-known as “chiral bilayer effect”.¹² As



Scheme 1 Chemical structure of *N*-octyl-D-gluconamide (8-GA). The arrows represent both the sequential group motion and the dehydration directions in the gelation process according to 2DCos results.

The Key Laboratory of Molecular Engineering of Polymers, Ministry of Education, Department of Macromolecular Science, Laboratory of Advanced Materials, Fudan University, Shanghai, 200433, China. E-mail: peiyiwu@fudan.edu.cn

† Electronic supplementary information (ESI) available. See DOI: 10.1039/c1sm05548h

reported, this effect is caused by the slowness of rearrangements from tail-to-tail hydrophobic bilayers to head-to-tail crystals. Further structural functionalization of gluconamides can produce organogels,¹³ which have even been used in liquid crystalline physical gels.¹⁴

Several researches have been devoted to explore the molecular origin of the bilayer helical assemblies of 8-GA, both by theoretical calculations¹⁵ and experimental observations.¹⁶ Obviously, there are three competing forces in the gelation process corresponding to three binding sites: hydrophobic interactions of octyl chains inclined to form spherical micelles, hydrogen bonding of amide linkages inclined to transform the spheres to discs, and the chiral bilayer stabilizing effect of open-chain carbohydrate head groups.¹⁷ However, nearly all the previous studies were focused on structural characterization of gels and corresponding crystals. To the best of our knowledge, no investigations concerning the evolving gelation process or the microdynamic mechanism have ever been reported. But it is really helpful to understand the assembly phenomenon of gelators because most gel systems are in a metastable state and hence their formation is governed by thermodynamics and kinetics. What's more, solvents also involve the gelation process, but the role of them is still poorly understood.¹⁸

In this paper, near infrared (NIR) spectroscopy was employed to trace both the spectral variations of 8-GA and solvent in the dynamic gelation process upon cooling. Additionally, two-dimensional correlation spectroscopy (2Dcos)¹⁹ in combination with perturbation correlation moving window (PCMW)²⁰ technique was used to obtain information of sequential group motions to further illustrate the final microdynamic mechanism.

2 Experimental section

2.1 Materials

8-GA was obtained by aminolysis of D-glucono- δ -lactone with n-octylamine (both from Aladdin Co. Ltd.) in methanol as described in literature.^{9a} The concentration of 8-GA aqueous solution was fixed to be 30wt%.

2.2 Instruments and measurements

Calorimetric measurements were performed on a Mettler-Toledo differential scanning calorimeter thermal analyzer. The sample of 8-GA solution for FT-NIR measurements was prepared by being sealed in the sample cell (quartz glass, 1 mm width). The FT-NIR measurements were performed on a Nicolet Nexus 470 spectrometer with a spectral resolution of 4 cm^{-1} and 32 scans were accumulated to obtain an acceptable signal-to-noise ratio. The spectra were recorded in a variable temperature cell between 80 and 64 $^{\circ}\text{C}$ in intervals of 1 $^{\circ}\text{C}$ with an accuracy of 0.1 $^{\circ}\text{C}$.

2.3 Investigation methods

Perturbation correlation moving window (PCMW). FT-NIR spectra collected with an increment of 1 $^{\circ}\text{C}$ during cooling were used to perform 2D correlation analysis. Primary data processing was carried out with the method Morita provided and further correlation calculation was performed using the software 2D Shige, ver. 1.3 (© Shigeaki Morita, Kwansai-Gakuin University,

Japan, 2004–2005). The final contour maps were plotted by Origin program, ver. 8.1, with warm colors (red and yellow) defined as positive intensities and cool colors (blue) as negative ones. An appropriate window size ($2m + 1 = 9$) was chosen to generate PCMW spectra with good quality.

2D correlation spectroscopy (2Dcos). FT-NIR spectra used for PCMW analysis were also used to perform 2D correlation analysis. 2D correlation analysis was carried out using the same software 2D Shige ver. 1.3 (© Shigeaki Morita, Kwansai-Gakuin University, Japan, 2004–2005), and was further plotted into the contour maps by Origin program ver. 8.0. In the contour maps, warm colors (red and yellow) are defined as positive intensities, while cool colors (blue) as negative ones.

3 Results and discussion

3.1 Conventional NIR

The whole gelation process of 8-GA was *in situ* monitored by NIR spectroscopy upon cooling from 80 to 64 $^{\circ}\text{C}$ (Fig. 1). For clarity, only a 2 $^{\circ}\text{C}$ interval is shown here. Two spectral regions are mainly focused in this paper: NH- and OH-related overtones (7345 – 6035 cm^{-1}) and CH-related overtones (5940 – 5620 cm^{-1}). The former region contributes from N–H in the amide linkage of 8-GA and O–H from chiral carbohydrate head groups as well as the solvent. The latter one all arises from C–H groups in 8-GA

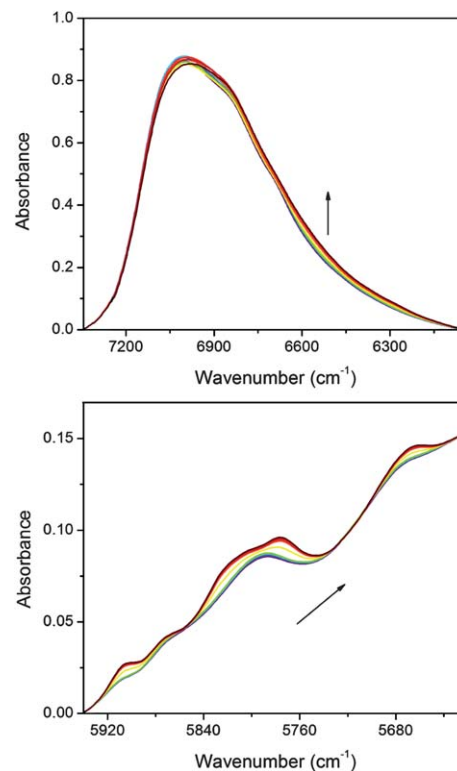


Fig. 1 Temperature-dependent overlaid NIR spectra of 8-GA in water (30wt%) during gelation upon cooling from 80 to 64 $^{\circ}\text{C}$. For clarity, only a 2 $^{\circ}\text{C}$ interval is shown here. The arrows represent the main tendency of spectral variations.

skeletons. Thus nearly all the group motions of the gelator and solvent can be primarily traced by NIR spectroscopy.

From Fig. 1, obvious spectral changes can be observed. NH-related overtones from 8-GA at lower frequencies show continuous increase during cooling, while all CH-related overtones show similar spectral increase in combination with apparent band shift and band splitting. The band shift of CH-related overtones can be explained by a hydrophobic interaction with neighboring water molecules of the solution. The higher the number of water molecules surrounding C–H groups is, the higher the vibrational frequency is.²¹ Similar phenomenon can be easily found in the coil-to-globule phase transition of poly(*N*-isopropylacrylamide) in water.²² It reveals that the octyl chains of 8-GA experienced a dehydration process during gelation.

Upon cooling, the band at 5795 cm⁻¹ continuously splits into two bands at 5824 and 5772 cm⁻¹, which all come from the vibrational overtones of octyl chains. As reported,^{4a,17} at the temperature above the gelation point (T_{gel}), 8-GA molecules are inclined to form spherical micelles in which all NH and OH groups are hydrated outside while hydrophobic octyl chains are inside. Although the cross-section structure of spherical micelles seems to be similar to the structure of micellar fibers after gel formation, our NIR analysis shows that the conformation of hydrophobic octyl chains in micellar fibers are much more ordered than that in spherical micelles, which can only explain the C-position-induced band splitting of C–H groups surrounded by water molecules. This result is also in good conformity with previous judgement about the “tight hydrophobic cores” in curved bilayer superstructures.¹¹

To examine the spectral variations to further determine T_{gel} , temperature-dependent integral absorption of NH-related overtones as well as CH-related overtones of 8-GA have been presented in Fig. 2. Interestingly, all the points obey S-shaped variations, thus Boltzmann fitting method was employed for an accurate determination of the transition temperature. The corresponding equation is as follows:

$$y = \frac{A_1 - A_2}{1 + e^{(x-x_0)/dx}} + A_2 \quad (1)$$

In eqn (1), A_1 is the minimum value of the function; A_2 is the maximum value of the function; x_0 is the value on the x axis corresponding to the inflection of the curve, which also equals to the transition temperature; and dx is the domain where this value lies.²³ Therefore T_{gel} can be determined to be 71.1 °C for NH-related overtones and 72.2 °C for CH-related overtones, which are all close to DSC results (66.7 °C, shown in the ESI).† Thus we can preliminarily conclude that CH-related dehydration occurs earlier than NH-related hydrogen bonding changes.

3.2 Perturbation correlation moving window

PCMW is a newly developed technique, whose basic principles can date back to conventional moving window proposed by Thomas.^{20a} Later in 2006, Morita^{20b} improved this technique to much wider applicability through introducing the perturbation variable into correlation equation. In addition to its original ability in determining transition points as conventional moving window did, PCMW can additionally monitor complicated spectral variations along the perturbation direction.

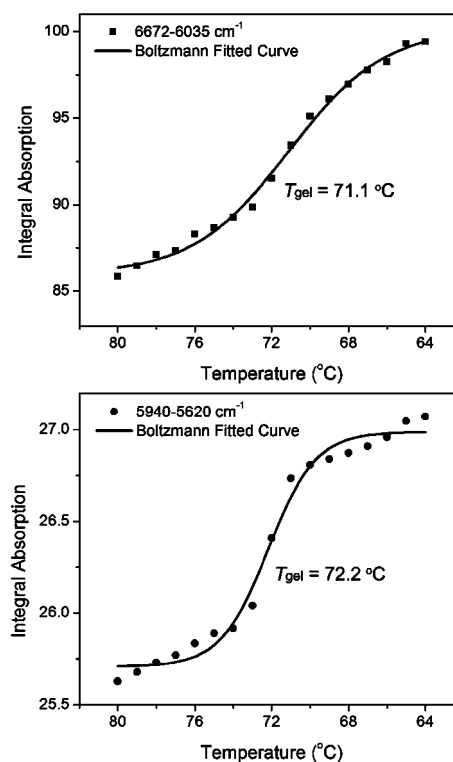


Fig. 2 Temperature-dependent integral absorption of 8-GA in the regions 6672–6035 cm⁻¹ and 5940–5620 cm⁻¹ respectively during gelation. The solid lines represent Boltzmann fitted curves.

Fig. 3 presents PCMW synchronous and asynchronous spectra of 8-GA during cooling from 80 to 64 °C. PCMW synchronous spectra are very helpful to find transition points. Thus for NH-related overtones, $T_{\text{gel}} \sim 71$ °C, and for CH-related overtones, $T_{\text{gel}} \sim 72$ °C. The gel formation temperatures obtained by

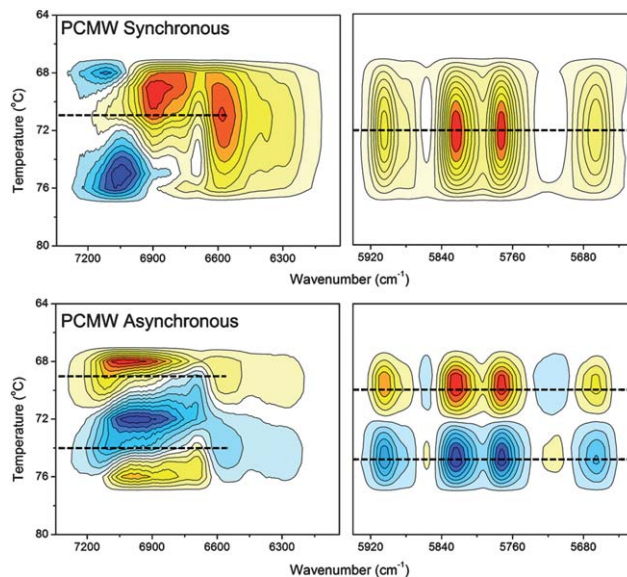


Fig. 3 PCMW synchronous and asynchronous spectra of 8-GA generated from all the spectra between 80 and 64 °C. Wherein, warm colors (red and yellow) are defined as positive intensities, while cool colors (blue) as negative ones.

PCMW are almost the same to Boltzmann fitting results, and once again we can conclude CH-related dehydration has an earlier response during gelation process.

In addition to determine transition points, PCMW can also monitor the spectral variations along temperature perturbation combining the signs of synchronous and asynchronous spectra by the following rules: positive synchronous correlation represents spectral intensity increasing, while negative one represents decreasing; positive asynchronous correlation can be observed for a convex spectral intensity variation while negative one can be observed for a concave variation.^{20b} Based on this point, we can ascertain that both NH- and CH-related overtones of 8-GA show an S-shaped spectral increase, consistent with the above conventional NIR analysis. The transition temperature region can also be determined by the peaks in asynchronous spectra which are all turning points of the S-shaped curves. Then we can conclude that 8-GA form entangled gels mainly between 70 and 75 °C. Note that although to obtain the transition temperature and region is important for gelators, it is usually very hard by DSC measurements due to apparent solvent evaporation but often roughly estimated by a tube inversion method. PCMW proves to be a feasible method. It is also notable that OH-related overtones at higher frequencies contributing from both chiral head groups of 8-GA and large amounts of water in the system are hardly distinguished by PCMW. Thus we would not discuss the spectral variations of OH-related overtones in detail in this section.

3.3 Two-dimensional correlation analysis

2Dcos is a mathematical method whose basic principles were first proposed by Noda in 1986.^{19a} Up to the present, 2Dcos has been widely used to study spectral variations of different chemical species under various external perturbations (*e.g.* temperature, pressure, concentration, time, electromagnetic, *etc.*)^{19b} Due to the different response of different species to external variables, additional useful information about molecular motions or conformational changes can be extracted which cannot be obtained straight from conventional 1D spectra.

All the spectra during gel formation process between 80 and 64 °C were used to perform 2D correlation analysis, as shown in Fig. 4. Two spectra, synchronous and asynchronous spectra, can also be generated. 2D synchronous spectra reflect simultaneous changes between two given wavenumbers. The bands at 6880, 6763, 6580, 5907, 5824, 5772, 5664 cm⁻¹ all have positive cross-peaks, indicating that they had similar response of spectral intensities to temperature perturbation—that is, all increase during cooling determined from raw spectra. On the other hand, the bands at 7076 cm⁻¹ have negative cross-peaks with all the other bands, indicating spectral intensities decrease during cooling.

2D asynchronous spectra can significantly enhance the spectral resolution. In Fig. 4, many subtle bands have been identified, such as the splitting bands at 5811, 5758 cm⁻¹ attributed from 2ν_{as}(CH₂) of octyl chains in the gel state. For the convenience of discussion, all the bands found in asynchronous spectra and their corresponding assignments are presented in Table 1.

Except for enhancing spectral resolution, 2D correlation spectroscopy can also discern the specific order taking place under external perturbation. An asynchronous cross-peak can

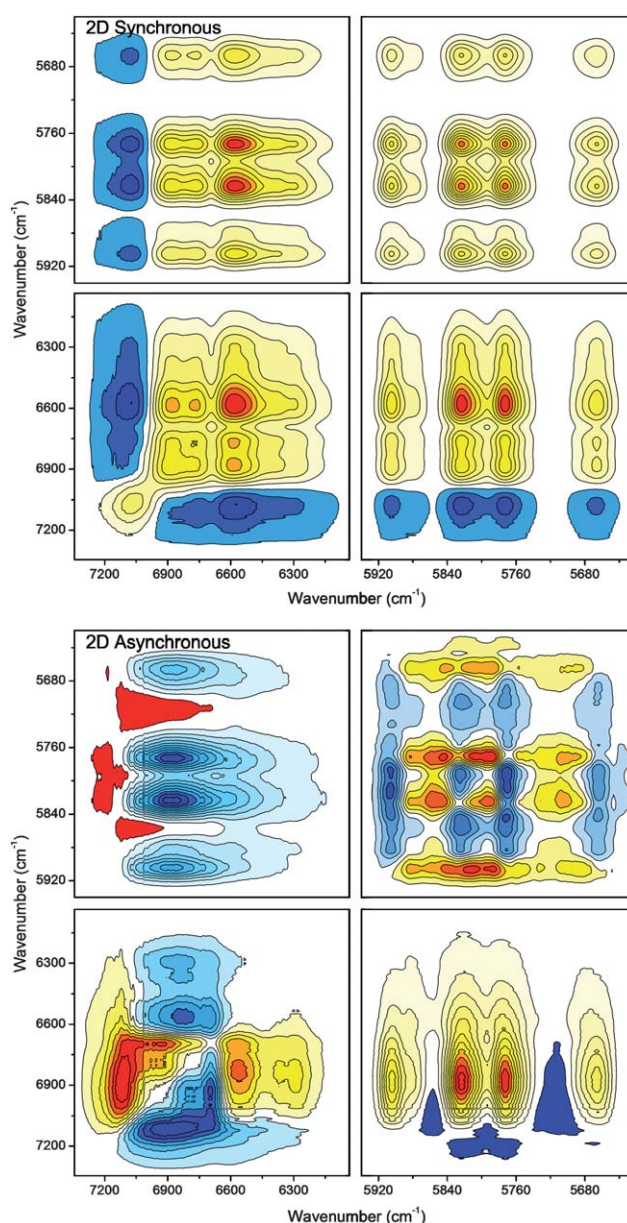


Fig. 4 2D synchronous and asynchronous spectra of 8-GA generated from all the spectra between 80 and 64 °C. Wherein, warm colors (red and yellow) are defined as positive intensities, while cool colors (blue) as negative ones.

develop only if the intensities of two spectral features change out of phase with each other (*i.e.*, delayed or accelerated if time is the external variable). The judging rule can be summarized as Noda's rule—that is, if the cross-peaks (ν_1 , ν_2 , and assume $\nu_1 > \nu_2$) in synchronous and asynchronous spectra have the same sign, the change at ν_1 may occur prior to that of ν_2 , and vice versa. As space is limited, the determination details of sequential orders have been presented in supporting information, and only the final specific order is given as follows (\rightarrow means prior to or earlier than): 5859 cm⁻¹ \rightarrow 5843 cm⁻¹ \rightarrow 5795 cm⁻¹ \rightarrow 5884 cm⁻¹ \rightarrow 5685 cm⁻¹ \rightarrow 5811 cm⁻¹ \rightarrow 5758 cm⁻¹ \rightarrow 5824 cm⁻¹ \rightarrow 5772 cm⁻¹ \rightarrow 5664 cm⁻¹ \rightarrow 5907 cm⁻¹ \rightarrow 6295 cm⁻¹ \rightarrow 6561 cm⁻¹ \rightarrow 5708 cm⁻¹ \rightarrow 6912 cm⁻¹ \rightarrow 6856 cm⁻¹ \rightarrow 6698 cm⁻¹ \rightarrow 7116 cm⁻¹. That is, 2ν_{as}(C–H in C⁸H₃) \rightarrow 2ν_{as}(C–H in C^{2'-7'}H₂)

Table 1 Tentative band assignments of 8-GA according to 2Dcos during gel formation process. Corresponding mid-IR spectra can be consulted in the ESI

Wavenumber (cm ⁻¹)	Assignments
7116	2ν(O–H in water)
6912	Self-associated 2ν(O–H in 8-GA)
6856	
6698	H-bonded with water
6561	H-bonded with C=O
6295	H-bonded with water
5907	2ν _{as} (C–H in C ¹ H ₂)
5884, 5859, 5843	2ν _{as} (C–H in C ⁸ H ₃)
5824, 5811, 5772, 5758	In gel 2ν _{as} (C–H in C ^{2–7} H ₂)
5795	In solution
5708	2ν(C–H in C ^{1–5} H)
5685	Hydrated 2ν _s (C–H in C ^{2–7} H ₂)
5664	Dehydrated

(in solution) → 2ν_s(C–H in C^{2–7}H₂) (hydrated) → 2ν_{as}(C–H in C^{2–7}H₂) (in gel) → 2ν_s(C–H in C^{2–7}H₂) (dehydrated) → 2ν_{as}(C–H in C¹H₂) → 2ν(N–H in 8-GA) (H-bonded with water) → 2ν(N–H in 8-GA) (H-bonded with C=O) → 2ν(C–H in C^{1–5}H) → 2ν(O–H in 8-GA) (self-associated) → 2ν(O–H in 8-GA) (H-bonded with water) → 2ν(O–H in water).

Not considering different vibrational modes and states (gel or solution, hydrated or dehydrated, and H-bonding types), we always have C⁸H₃ → C^{2–7}H₂ → C¹H₂ → N–H → C^{1–5}H → O–H in 8-GA → O–H in water. It is notable that during the gelation process of 8-GA, all group motions have a continuous transfer from the octyl tail to the chiral carbohydrate head through amide linkage followed by the final immobilization of the solvent. This transfer of groups motions can be interpreted to the sequential or successive response of specific groups (reflected by changes of spectral intensities) to the cooling temperature. That means the octyl tail has an earlier response to temperature than amide linkage and chiral carbohydrate head during the gelation process. Judging from earlier conventional NIR analysis, this response is actually a dehydration process. Therefore, we can conclude that the driving force of the gelation process in microdynamics can only be the dehydration process of hydrophobic octyl chains, which have not been paid enough attention in previous studies. Due to the late response upon cooling, chiral carbohydrate head has an obvious stabilizing effect on the gel state, which can be attributed to the “chiral bilayer effect”,¹² responsible for the formation of helical aggregates. As the linkage both structurally and in group motions, hydrogen bonding of amide groups are also essential for the formation of much ordered bilayer superstructures. As reported, no gel can be formed in *N*-methylated 8-GA.^{9a}

Now we turn to examine the effect of solvent on the conformation changes of 8-GA. The hydrophobic octyl chains experienced an obvious dehydration process, which have been discussed in conventional NIR analysis. The amide linkages have a transformation of hydrogen bonds from N–H...OH₂ to N–H...O=C ones, resulting in a more contact assembly. Actually, this is also a dehydration process. For chiral carbohydrate head groups, OH would absorb more water in the gel state upon cooling than in solution as the sequence order of 2ν(O–H in 8-GA) (self-associated) is prior to 2ν(O–H in 8-GA) (H-bonded with water). It is feasible that the obtained curved bilayer fibers

have larger surface than spherical micelles to be surrounded by more water molecules, which may also account for the too large surface energy to make the helices stable.^{10b}

Therefore, we can draw a conclusion that the gelation process of 8-GA upon cooling can be described in microdynamics as follows: all group motions have a continuous transfer from the octyl tail to the chiral carbohydrate head followed by the final immobilization of the solvent, which meanwhile, is actually a continuous dehydration process from the hydrophobic core to the outer hydrophilic chiral head. Both the two directions have been presented in Scheme 1.

Conclusions

In this paper, NIR spectroscopy in combination with 2Dcos and PCMW is employed to illustrate the gelation microdynamic mechanism of 8-GA in water. Two regions involving NH-, OH- and CH-related overtones are focused on to trace nearly all the group motions of 8-GA upon cooling. According to conventional NIR analysis, all CH-related overtones exhibit an apparent band shift to lower frequencies and a band splitting phenomenon. It reveals that the octyl chains of 8-GA experienced a dehydration process during gel formation resulting in a much tight and ordered hydrophobic core. Boltzmann fitting and PCMW have determined the transition temperature to be *ca.* 72 °C and the gelation temperature range 70–75 °C. According to 2Dcos results, we obtained such sequential orders as follows: C⁸H₃ → C^{2–7}H₂ → C¹H₂ → N–H → C^{1–5}H → O–H in 8-GA → O–H in water. Thus the gelation microdynamic mechanism of 8-GA can be concluded that all the group motions have a continuous transfer from the octyl tail to the chiral carbohydrate head followed by the final immobilization of the solvent, which meanwhile, is actually a continuous dehydration process from the hydrophobic core to the outer hydrophilic chiral head.

Acknowledgements

This work was financially supported by National Science Foundation of China (NSFC) (No. 20934002, 51073043) and the National Basic Research Program of China (No. 2009CB930000).

References

- (a) Y. Lin, Y. Qiao, C. Gao, P. Tang, Y. Liu, Z. Li, Y. Yan and J. Huang, *Chem. Mater.*, 2010, **22**, 6711–6717; (b) J. C. Tiller, *Angew. Chem., Int. Ed.*, 2003, **42**, 3072–3075; (c) K. Y. Lee and D. J. Mooney, *Chem. Rev.*, 2001, **101**, 1869–1880.
- L. A. Estroff and A. D. Hamilton, *Chem. Rev.*, 2004, **104**, 1201–1218.
- K. Hanabusa, M. Yamada, M. Kimura and H. Shirai, *Angew. Chem., Int. Ed. Engl.*, 1996, **35**, 1949–1951.
- (a) G. Li, W. Fudickar, M. Skupin, A. Klyszcz, C. Draeger, M. Lauer and J. H. Fuhrhop, *Angew. Chem., Int. Ed.*, 2002, **41**, 1828–1852; (b) H. Y. Lee, S. R. Nam and J. I. Hong, *Chem.–Asian J.*, 2009, **4**, 226–235.
- (a) T. Lin, R. Ho, C. Sung and C. Hsu, *Chem. Mater.*, 2008, **20**, 1404–1409; (b) J. Cu, Y. Zheng, Z. Shen and X. Wan, *Langmuir*, 2010, **26**, 15508–15515; (c) Y. Lin, A. Wang, Y. Qiao, C. Gao, M. Drechsler, J. Ye, Y. Yan and J. Huang, *Soft Matter*, 2010, **6**, 2031–2036.
- (a) J. Jung, J. Rim, E. Cho, S. Lee, I. Jeong, N. Kameda, M. Masuda and T. Shimizu, *Tetrahedron*, 2007, **63**, 7449–7456; (b) A. Meister, S. Drescher, G. Karlsson, G. Hause, U. Baumeister, G. Hempel, V. M. Garamus, B. Dobner and A. Blume, *Soft Matter*, 2010, **6**, 1317–1324.

- 7 (a) F. M. Menger, H. Zhang, K. L. Caran, V. A. Seredyuk and R. P. Apkarian, *J. Am. Chem. Soc.*, 2002, **124**, 1140–1141; (b) B. V. Shankar and A. Patnaik, *J. Phys. Chem. B*, 2007, **111**, 9294–9300.
- 8 D. Jang, H. Y. Lee, M. Park, S. R. Nam and J. I. Hong, *Chem. Eur. J.*, 2010, **16**, 4836–4842.
- 9 (a) B. Pfannemüller and W. Welte, *Chem. Phys. Lipids*, 1985, **37**, 227–240; (b) B. Pfannemüller and I. Kuhn, *Makromol. Chem.*, 1988, **189**, 2433–2442; (c) J. H. Fuhrhop, P. Schnieder, E. Boekema and W. Helfrich, *J. Am. Chem. Soc.*, 1988, **110**, 2861–2867.
- 10 (a) J. Koenig, C. Boettcher, H. Winkler, E. Zeitler, Y. Talmon and J. H. Fuhrhop, *J. Am. Chem. Soc.*, 1993, **115**, 693–700; (b) J. H. Fuhrhop, T. Wang, S. Bhosale and M. Lauer, in *Molecular Gels*, (Eds: R. G. Weiss, P. Terech), Springer, Netherlands, 2006, pp. 649–664.
- 11 J. H. Fuhrhop, S. Svenson, C. Boettcher, E. Rossler and H. M. Vieth, *J. Am. Chem. Soc.*, 1990, **112**, 4307–4312.
- 12 J. H. Fuhrhop, P. Schnieder, J. Rosenberg and E. Boekema, *J. Am. Chem. Soc.*, 1987, **109**, 3387–3390.
- 13 R. Hafkamp, M. Feiters and R. Nolte, *J. Org. Chem.*, 1999, **64**, 412–426.
- 14 (a) K. Yabuuchi, A. Rowan, R. Nolte and T. Kato, *Chem. Mater.*, 2000, **12**, 440–443; (b) T. Kato, Y. Hirai, S. Nakaso and M. Moriyama, *Chem. Soc. Rev.*, 2007, **36**, 1857–1867.
- 15 N. Nandi and B. Bagchi, *J. Am. Chem. Soc.*, 1996, **118**, 11208–11216.
- 16 (a) S. Svenson, B. Kirste and J. H. Fuhrhop, *J. Am. Chem. Soc.*, 1994, **116**, 11969–11975; (b) S. Svenson, J. Koenig and J. H. Fuhrhop, *J. Phys. Chem.*, 1994, **98**, 1022–1028; (c) C. Boettcher, H. Stark and M. van Heel, *Ultramicroscopy*, 1996, **62**, 133–139; (d) I. Sack, S. Macholl, J. H. Fuhrhop and G. Buntkowsky, *Phys. Chem. Chem. Phys.*, 2000, **2**, 1781–1788.
- 17 J. H. Fuhrhop, D. Spiroski and P. Schnieder, *React. Polym.*, 1991, **15**, 215–220.
- 18 J. H. van Esch, *Langmuir*, 2009, **25**, 8392–8394.
- 19 (a) I. Noda, *Bull. Am. Phys. Soc.*, 1986, **31**, 520–528; (b) I. Noda, *J. Mol. Struct.*, 2008, **883–884**, 2–26.
- 20 (a) M. Thomas and H. H. Richardson, *Vib. Spectrosc.*, 2000, **24**, 137–146; (b) S. Morita, H. Shinzawa, I. Noda and Y. Ozaki, *Appl. Spectrosc.*, 2006, **60**, 398–406.
- 21 P. Schmidt, J. Dybal and M. Trchová, *Vib. Spectrosc.*, 2006, **42**, 278–283.
- 22 (a) B. Sun, Y. Lin, P. Wu and H. Siesler, *Macromolecules*, 2008, **41**, 1512–1520; (b) S. Sun, J. Hu, H. Tang and P. Wu, *J. Phys. Chem. B*, 2010, **114**, 9761–9770; (c) S. Sun and P. Wu, *Macromolecules*, 2010, **43**, 9501–9510.
- 23 M. C. Popescu, D. Filip, C. Vasile, C. Cruz, J. M. Rueff, M. Marcos, J. L. Serrano and G. Singurel, *J. Phys. Chem. B*, 2006, **110**, 14198–14211.